

Hg₃(Te₃O₈)(SO₄): A New Sulfate Tellurite with Novel Structure and Large Birefringence Explored from d¹⁰ Metal Compounds

Peng-Fei Li^{a,b}, Chun-Li Hu^a, Ya-Ping Gong^a, Fang Kong^{*,a}, Jiang-Gao Mao^a

^a State Key Laboratory of Structural Chemistry, Fujian Institute of Research on the Structure of Matter, Chinese Academy of Sciences, Fuzhou 350002, P. R. China.

^b College of Chemical Engineering, Fuzhou University, Fuzhou, Fujian 350116, P. R. China.

E-mail: kongfang@fjirsm.ac.cn;

Supporting Information

S1. Experimental Section.....	2
S2. Single-crystal X-ray diffraction.....	3
S3. Computational Method.....	3
Table S1 Summary of crystal data and structural refinements for the four compounds.....	5
Table S2 Calculated bond valences for the four compounds.....	6
Table S3 The state energies (eV) of the lowest conduction band (L-CB) and the highest valence band (H-VB) of the four compounds.	9
Figure S1. Simulated and experimental XRD powder patterns of Ga ₂ (TeO ₃)(SO ₄)(OH) ₂ (a), Zn ₄ (Te ₃ O ₇) ₂ (SO ₄) ₂ (H ₂ O) (b) and Hg ₃ (Te ₃ O ₈)(SO ₄) (c).	10
Figure S2. View of the layered structure of Ga ₂ (TeO ₃)(SO ₄)(OH) ₂ along c- (a) and a-axis (b).	11
Figure S3. The indium oxide layer of In ₂ (TeO ₃) ₂ (SO ₄)(H ₂ O).	11
Figure S4. The [Zn ₄ (SO ₄) ₂ (H ₂ O)] ⁴⁺ cluster in Zn ₄ (Te ₃ O ₇) ₂ (SO ₄) ₂ (H ₂ O).	12
Figure S5. The coordination modes of Hg(1), Hg(2) and Hg(3) (b), the Te ₃ O ₈ trimer (a), and the mercury oxide chains and layer (c) of Hg ₃ (Te ₃ O ₈)(SO ₄).	13
Figure S6. The ladder-shaped double chain structure in Tl ₂ (Te ₃ O ₇) (a), the zigzag chain in Fe(Te ₃ O ₇)X (X = Cl, Br) (b), the 2D layered structure in Ba(Te ₃ O ₇) (c).	14
Figure S7. TGA and DSC curves of Ga ₂ (TeO ₃)(SO ₄)(OH) ₂ (a), Zn ₄ (Te ₃ O ₇) ₂ (SO ₄) ₂ (H ₂ O) (b) and Hg ₃ (Te ₃ O ₈)(SO ₄) (c).	15
Figure S8. IR spectra of Ga ₂ (TeO ₃)(SO ₄)(OH) ₂ (a), Zn ₄ (Te ₃ O ₇) ₂ (SO ₄) ₂ (H ₂ O) (b) and Hg ₃ (Te ₃ O ₈)(SO ₄) (c).	16
Figure S9. UV-Vis-NIR diffuse reflectance spectrum of Ga ₂ (TeO ₃)(SO ₄)(OH) ₂ (a), Zn ₄ (Te ₃ O ₇) ₂ (SO ₄) ₂ (H ₂ O) (b) and Hg ₃ (Te ₃ O ₈)(SO ₄) (c).	17
Figure S10. Calculated band structures of the four compounds.	18
Figure S11. Calculated total and partial density of states for the four compounds.	19
Figure S12. Calculated refractive indices and birefringence of the four compounds.	20
Figure S13. Calculated refractive (n) and birefringence (Δn) indices of In ₂ (TeO ₃)(SO ₄)(OH) ₂ (H ₂ O) and In ₃ (TeO ₃)(SO ₄)F ₃ (H ₂ O).	21
References.....	22

S1. Experimental Section

Materials and Instrumentations.

All the chemicals were analytically pure from commercial sources and used without further purification: TeO₂ (Aladdin, >99.99%, AR), HgO (Tansoole, >99%, AR), ZnO (Aladdin, >99.99%, AR), Ga₂O₃ (Aladdin, 99.9%, AR), In₂O₃ (Aladdin, 99.9%, AR), H₂SO₄ (Sinopharm, 95.0~98.0%, AR). Powder X-ray diffraction (PXRD) patterns of the three compounds were collected on the Miniflex 600 powder X-ray diffractometer using Cu K α radiation at room temperature in the angular range of $2\theta = 5-70^\circ$ with a scan step size of 0.02° . IR spectra were carried out on a Magna 750 FT-IR spectrometer using air as background in the range of $4000-400\text{ cm}^{-1}$ with a resolution of 2 cm^{-1} at room temperature. The UV-vis-NIR spectra were obtained at $2000-200\text{ nm}$ by a PerkinElmer Lambda 900 spectrophotometer using BaSO₄ as the reference, and the reflection spectra were converted into an absorption spectrum using the Kubelka-Munk function. Thermogravimetric analyses (TGA) and differential scanning calorimetry (DSC) were measured by Netzsch STA 499C installation. The samples about 2.0-5.0 mg were placed in alumina crucibles and heated in $25-1200\text{ }^\circ\text{C}$ at a rate of $15\text{ }^\circ\text{C}/\text{min}$ under N₂ atmosphere.

Syntheses

The four compounds were obtained by mild hydrothermal reactions. The component parts are as follows: TeO₂ (0.319 g, 2 mmol), Ga₂O₃ (0.187 g, 1.0 mmol), H₂SO₄ (0.20 mL) and H₂O (2.5 mL) for **Ga₂(TeO₃)(SO₄)(OH)₂**; TeO₂ (0.319 g, 2 mmol), In₂O₃ (0.277 g, 1.0 mmol), H₂SO₄ (0.20 mL) and H₂O (2.5 mL) for **In₂(SO₄)(TeO₃)(OH)₂(H₂O)**; TeO₂ (0.319 g, 2 mmol), ZnO (0.081 g, 1.0 mmol), H₂SO₄ (0.20 mL) and H₂O (2.5 mL) for **Zn₄(Te₆O₁₄)(SO₄)₂(H₂O)**; TeO₂ (0.160 g, 1 mmol), HgO (0.325 g, 1.5 mmol), H₂SO₄ (0.15 mL) and H₂O (3 mL) for **Hg₃(Te₃O₈)(SO₄)**. The mixtures were sealed in an autoclave equipped with a Teflon liner (23 mL), which were heated to $220\text{ }^\circ\text{C}$ to generate autogenous pressures in 5 h and held for 4 days, followed by cooling to $30\text{ }^\circ\text{C}$ at a rate of $3\text{ }^\circ\text{C}/\text{h}$. The products were washed with alcohol and dried in air at room temperature. Transparent crystals of **Ga₂(TeO₃)(SO₄)(OH)₂**, **Zn₄(Te₃O₇)₂(SO₄)₂(H₂O)** and **Hg₃(Te₃O₈)(SO₄)**, were obtained in yields of 28%, 52% and 35% (based on Te) respectively. The yield of

$\text{In}_2(\text{SO}_4)(\text{TeO}_3)(\text{OH})_2(\text{H}_2\text{O})$ is very low, only several small crystals can be isolated. Powder X-ray diffraction on the polycrystalline samples were in good agreement with the generated patterns from the single crystal structures (Figure S1).

S2. Single-crystal X-ray diffraction

Data collections for the three compounds were performed on Agilent Technologies SuperNova Dual Wavelength CCD diffractometer with a graphite-monochromated Mo-K α radiation ($\lambda = 0.71073 \text{ \AA}$). The structures were solved by direct methods and refined by full-matrix least-squares fitting on F^2 using *SHELXTL-97* crystallographic software package. All of the atoms were refined with anisotropic thermal parameters and finally converged for $F_0^2 \geq 2\sigma(F_0^2)$. The structural data were also checked for possible missing symmetry with the program PLATON, and no higher symmetry was found. The crystallographic data and refinement details for the compounds are given in Table S1. The selected bond lengths are listed in Table S2.

S3. Computational Method

Single-crystal structural data of the four compounds were used for the theoretical calculations. The electronic structures were performed using a plane-wave basis set and pseudo-potentials within density functional theory (DFT) implemented in the total-energy code CASTEP [1]. For the exchange and correlation functional, we chose Perdew–Burke–Ernzerhof (PBE) in the generalized gradient approximation (GGA) [2]. The interactions between the ionic cores and the electrons were described by the ultrasoft pseudopotential [3]. The following valence-electron configurations were considered in the computation: Ga-3d¹⁰4s²4p¹, In-5s²5p¹, Zn-3d¹⁰3p²4s², Hg-5d¹⁰5p²6s², Te-5s²5p⁴, O-2s²2p⁴, S-3s²3p⁴ and H-1s¹. The numbers of plane waves included in the basis sets were determined by cutoff energy of 750 eV, 750 eV and 800 eV for the four compounds respectively. The numerical integration of the Brillouin zone was performed using Monkhorst-Pack k-point sampling of $5 \times 3 \times 4$, $2 \times 2 \times 1$, $4 \times 3 \times 3$ and $1 \times 5 \times 2$ for the four compounds respectively. The other parameters and convergent criteria were the default values of CASTEP code.

The calculations of linear optical properties in terms of the complex dielectric function $\epsilon(\omega) = \epsilon_1(\omega) + i\epsilon_2(\omega)$ were made. The imaginary part of the dielectric function ϵ_2 was given in the following equation:

$$\epsilon_2(\omega) = \frac{8\pi^2 h^2 e^2}{(m^2 V)} \sum_k \sum_{cv} (f_c - f_v) \frac{p_{cv}^i(k) p_{cv}^j(k)}{E_{vc}^2} \delta [E_c(k) - E_v(k) - \hbar\omega]$$

The f_c and f_v represent the Fermi distribution functions of the conduction and valence band. The term $p_{cv}^i(k)$ denotes the momentum matrix element transition from the energy level c of the conduction band to the level v of the valence band at the k th point in the Brillouin zone (BZ), and V is the volume of the unit cell.

The real part $\epsilon_1(\omega)$ of the dielectric function $\epsilon(\omega)$ follows from the Kramer–Kronig relationship. All the other optical constants may be derived from $\epsilon_1(\omega)$ and $\epsilon_2(\omega)$. For example, the refractive index $n(\omega)$ can be calculated using the following expression [4]:

$$n(\omega) = \frac{1}{\sqrt{2}} \left[\sqrt{\epsilon_1^2(\omega) + \epsilon_2^2(\omega)} + \epsilon_1(\omega) \right]^{1/2}$$

Table S1 Summary of crystal data and structural refinements for the four compounds.

molecular formula	Ga ₂ (TeO ₃)(SO ₄)(OH) ₂	In ₂ (TeO ₃) ₂ (SO ₄)(H ₂ O)	Zn ₄ (Te ₃ O ₇) ₂ (SO ₄) ₂ (H ₂ O)	Hg ₃ (Te ₃ O ₈)(SO ₄)
Formula Weight	445.12	694.92	1461.22	1208.64
crystal system	monoclinic	monoclinic	monoclinic	triclinic
space group	<i>P2₁/m</i>	<i>C2/c</i>	<i>C2/c</i>	<i>P-1</i>
Temperature(K)	99.97(17)	291(1)	290.55(10)	290.62(10)
F(000)	408	2464	2600	1016
a/Å	4.9825(7)	17.6356(14)	22.8452(16)	6.4986(6)
b/Å	9.7519(12)	6.7576(4)	5.4594(3)	9.7848(9)
c/Å	6.9741(10)	16.4550(12)	15.6547(13)	10.7128(10)
α(deg)	90.00	90.00	90.00	67.178(9)
β(deg)	93.550(12)	107.394(8)	99.598(7)	72.622(9)
γ(deg)	90.00	90.00	90.00	73.471(8)
V/Å ³	338.21(8)	1871.3(2)	1925.1(2)	588.10(9)
Z	2	8	4	2
Dc(g.cm ⁻³)	4.371	4.933	5.042	6.825
GOF on F ²	1.056	0.992	1.093	1.059
R ₁ ,wR ₂ [I > 2σ(I)] ^a	0.0345,0.0710	0.0246,0.0567	0.0289,0.0659	0.0398,0.0889
R ₁ , wR ₂ (all data) ^a	0.0448,0.0782	0.0289, 0.0598	0.0311,0.0672	0.0497,0.0958

^aR₁ = $\sum||F_o| - |F_c||/\sum|F_o|$, wR₂ = $\{\sum w[(F_o)^2 - (F_c)^2]^2/\sum w[(F_o)^2]^2\}^{1/2}$

Table S2 Calculated bond valences for the four compounds.

Compound	Bond	Bond	Bond-valence	BVS
		lengths		
Ga ₂ (TeO ₃)(SO ₄)(OH) ₂	Te(1)-O(1)#1	1.895(4)	1.245	3.575
	Te(1)-O(1)	1.895(4)	1.245	
	Te(1)-O(2)#2	1.949(6)	1.073	
	Te(1)···O(3)#2	2.609(4)	0.181	
	Te(1)···O(3)#3	2.609(4)	0.181	
	Ga(1)-O(1)	1.949(4)	0.553	3.230
	Ga(1)-O(1)#5	2.012(4)	0.468	
	Ga(1)-O(2)	1.932(3)	0.581	
	Ga(1)-O(3)#4	1.953(4)	0.546	
	Ga(1)-O(3)	1.983(4)	0.506	
	Ga(1)-O(4)	1.935(4)	0.576	6.133
	S(1)-O(4)#1	1.491(5)	1.433	
	S(1)-O(4)	1.491(5)	1.433	
	S(1)-O(5)	1.443(6)	1.627	
S(1)-O(6)	1.441(7)	1.640		
In ₂ (TeO ₃) ₂ (SO ₄)(H ₂ O)	Te(1)-O(1)	1.908(3)	1.205	3.907
	Te(1)-O(2)	1.889(3)	1.269	
	Te(1)-O(3)	1.844(3)	1.433	
	Te(2)-O(4)	1.872(3)	1.328	3.690
	Te(2)-O(6)	1.909(3)	1.202	
	Te(2)-O(5)	1.922(3)	1.160	
	In(1)-O(2)#1	2.201(3)	0.407	2.978
	In(1)-O(2)#2	2.207(3)	0.439	
	In(1)-O(3)	2.184(3)	0.467	
	In(1)-O(3)#1	2.550(4)	0.174	
	In(1)-O(5)#3	2.158(3)	0.501	
	In(1)-O(7)	2.237(4)	0.404	3.062
	In(1)-O(11)#4	2.100(4)	0.586	
	In(2)-O(1)#5	2.118(3)	0.558	
	In(2)-O(1)#6	2.215(3)	0.429	
	In(2)-O(4)	2.170(3)	0.485	
	In(2)-O(5)	2.212(3)	0.433	6.122
	In(2)-O(8)#7	2.122(4)	0.552	
	In(2)-O(11)	2.088(3)	0.605	
	S(1)-O(7)	1.468(4)	1.524	
S(1)-O(8)	1.487(4)	1.448	6.122	
S(1)-O(9)	1.460(4)	1.558		
S(1)-O(10)	1.452(4)	1.592		
Zn ₄ (Te ₃ O ₇) ₂ (SO ₄) ₂ (H ₂ O)	Te(1)-O(1)	1.851(4)	1.406	3.828

	Te(1)-O(2)	1.870(5)	1.335	3.734
	Te(1)-O(3)	1.946(4)	1.087	
	Te(2)-O(4)	2.022(5)	0.885	
	Te(2)-O(5)	1.931(4)	1.132	
	Te(2)-O(6)	1.901(4)	1.228	
	Te(2)-O(6)#1	2.242(5)	0.489	
	Te(3)-O(3)#2	2.104(5)	0.709	3.946
	Te(3)-O(4)	1.900(4)	1.231	
	Te(3)-O(5)#3	2.117(5)	0.685	
	Te(3)-O(8)	1.874(4)	1.321	
	Zn(1)-O(1)	2.020(5)	0.426	2.054
	Zn(1)-O(3)#4	2.169(4)	0.285	
	Zn(1)-O(7)	2.209(3)	0.255	
	Zn(1)-O(8)#5	2.079(5)	0.363	
	Zn(1)-O(10)#5	2.067(4)	0.375	
	Zn(1)-O(12)#6	2.092(5)	0.350	
	Zn(2)-O(2)	1.957(5)	0.505	1.810
	Zn(2)-O(5)#3	2.155(4)	0.296	
	Zn(2)-O(6)#7	1.953(4)	0.510	
	Zn(2)-O(8)	1.961(5)	0.499	
S(1)-O(9)	1.478(5)	1.484	6.003	
S(1)-O(9)	1.478(5)	1.484		
S(1)-O(10)	1.481(5)	1.472		
S(1)-O(11)	1.454(5)	1.583		
S(1)-O(12)	1.483(5)	1.464		
Hg ₃ (Te ₃ O ₈)(SO ₄)	Te(1)-O(1)	2.072(7)	0.774	3.882
	Te(1)-O(2)	1.881(7)	1.296	
	Te(1)-O(3)	1.864(9)	1.357	
	Te(1)-O(4)	2.268(8)	0.455	
	Te(2)-O(4)	1.909(8)	1.202	3.902
	Te(2)-O(5)	1.874(8)	1.321	
	Te(2)-O(6)	1.858(9)	1.379	
	Te(3)-O(1)	1.917(8)	1.176	4.004
	Te(3)-O(7)	1.838(9)	1.456	
	Te(3)-O(8)	1.860(8)	1.372	
	Te(3)-O(10)#1	2.601(8)	0.185	
	Hg(1)-O(1)#1	2.442(7)	0.251	1.713
	Hg(1)-O(2)#1	2.572(9)	0.176	
	Hg(1)-O(2)	2.287(10)	0.381	
	Hg(1)-O(3)#2	2.521(9)	0.202	
Hg(1)-O(3)	2.517(9)	0.205		
Hg(1)-O(4)#2	2.252(9)	0.419		

Hg(1)-O(6)#2	2.870(9)	0.079	
Hg(2)-O(3)	2.426(8)	0.262	2.065
Hg(2)-O(5)#2	2.723(10)	0.117	
Hg(2)-O(6)#2	2.609(8)	0.160	
Hg(2)-O(7)	2.137(9)	0.572	
Hg(2)-O(7)#3	2.472(8)	0.231	
Hg(2)-O(8)#4	2.111(9)	0.613	
Hg(2)-O(9)#5	2.743(10)	0.111	
Hg(3)-O(2)	2.466(8)	0.235	
Hg(3)-O(5)	2.099(8)	0.633	
Hg(3)-O(6)#6	2.086(8)	0.656	
Hg(3)-O(8)#7	2.490(10)	0.220	
Hg(3)-O(9)	2.621(9)	0.154	
S(1)-O(9)	1.466(10)	1.533	5.967
S(1)-O(10)	1.465(8)	1.537	
S(1)-O(11)	1.479(11)	1.480	
S(1)-O(12)	1.495(9)	1.417	

Symmetry transformations used to generate equivalent atoms:

For $\text{Ga}_2(\text{TeO}_3)(\text{SO}_4)(\text{OH})_2$: #1 $x, -y+1/2, z$; #2 $x+1, y, z$; #3 $x+1, -y+1/2, z$; #4 $-x, -y, -z+1$; #5 $-x-1, -y, -z+1$; #6 $x-1, y, z$

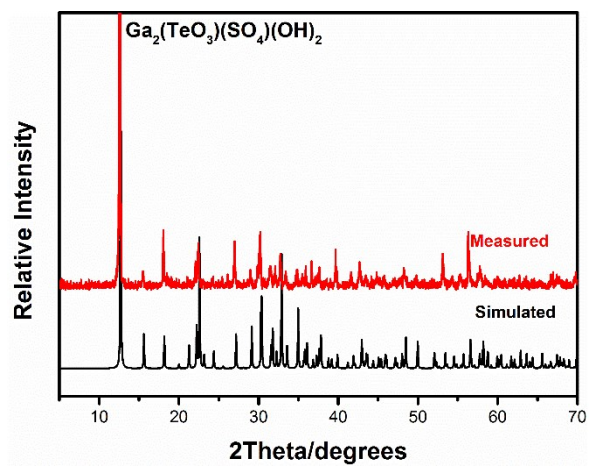
For $\text{In}_2(\text{TeO}_3)_2(\text{SO}_4)(\text{H}_2\text{O})$: #1 $-x+1/2, y+1/2, -z+1/2$; #2 $x, y+1, z$; #3 $x-1/2, y+1/2, z$; #4 $-x+1, y, -z+1/2$; #5 $x+1/2, y+1/2, z$; #6 $-x+1, -y+1, -z$; #7 $-x+1, -y+2, -z$

For $\text{Zn}_4(\text{Te}_6\text{O}_{14})(\text{SO}_4)_2(\text{H}_2\text{O})$: #1 $-x+1/2, -y+1/2, -z-1$; #2 $x, -y, z-1/2$; #3 $-x+1/2, y-1/2, -z-1/2$; #4 $x, y+1, z$; #5 $x, -y+1, z+1/2$; #6 $-x, -y+1, -z$; #7 $-x+1/2, y+1/2, -z-1/2$

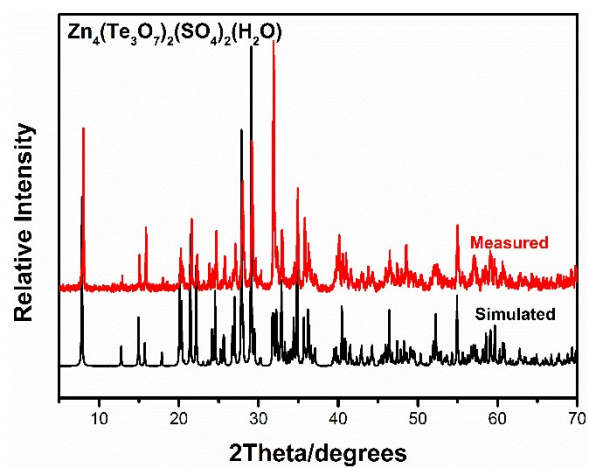
For $\text{Hg}_3(\text{Te}_3\text{O}_8)(\text{SO}_4)$: #1 $-x+1, -y+1, -z$; #2 $-x, -y+1, -z$; #3 $-x+1, -y+1, -z-1$; #4 $x-1, y, z$; #5 $x, y, z-1$; #6 $x+1, y, z$

Table S3 The state energies (eV) of the lowest conduction band (L-CB) and the highest valence band (H-VB) of the four compounds.

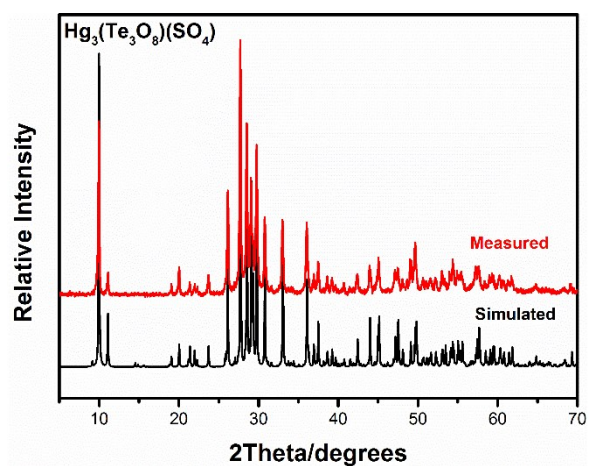
Compound	k-point	L-CB	H-VB
$\text{Ga}_2(\text{TeO}_3)(\text{SO}_4)(\text{OH})_2$	Z(0.000,0.000,0.500)	4.251806	-0.15029
	G(0.000,0.000,0.000)	4.20144	-0.04276
	Y(0.000,0.500,0.000)	4.04888	-0.09845
	A(-0.500,0.500,0.000)	4.08615	-0.02805
	B(-0.500,0.000,0.000)	4.139393	-0.00024
	D(-0.500,0.000,0.500)	4.062739	-0.00279
	E(-0.500,0.500,0.500)	4.038734	-0.01996
	C(0.000,0.500,0.500)	4.000253	-0.17692
$\text{In}_2(\text{TeO}_3)_2(\text{SO}_4)(\text{H}_2\text{O})$	L(-0.500,0.000,0.500)	2.78749	0
	M(-0.500,-0.500,0.500)	2.28126	-0.00221
	A(-0.500,0.000,0.000)	2.81736	-0.02240
	G(0.000,0.000,0.000)	2.30201	-0.03162
	Z(0.000,-0.500,0.500)	2.78748	0
	V(0.000,0.000,0.500)	2.31287	-0.05191
$\text{Zn}_4(\text{Te}_3\text{O}_7)_2(\text{SO}_4)_2(\text{H}_2\text{O})$	Z(0.000,0.000,0.500)	3.541378	-0.03716
	G(0.000,0.000,0.000)	3.540361	-0.0065
	Y(0.000,0.500,0.000)	3.535651	-0.05669
	A(-0.500,0.500,0.000)	3.530576	-0.04883
	B(-0.500,0.000,0.000)	3.55145	-0.00964
	D(-0.500,0.000,0.500)	3.545388	-0.04608
	E(-0.500,0.500,0.500)	3.558094	-0.04754
	C(0.000,0.500,0.500)	3.572216	-0.05551
$\text{Hg}_3(\text{Te}_3\text{O}_8)(\text{SO}_4)$	G(0.000,0.000,0.000)	2.467756	0
	F(0.000,0.500,0.000)	2.477729	-0.07055
	Q(0.000,0.500,0.500)	2.623512	-0.1444
	Z(0.000,0.000,0.500)	2.583891	-0.05208
	G(0.000,0.000,0.000)	2.467756	0



(a)



(b)



(c)

Figure S1. Simulated and experimental XRD powder patterns of $\text{Ga}_2(\text{TeO}_3)(\text{SO}_4)(\text{OH})_2$ (a), $\text{Zn}_4(\text{Te}_3\text{O}_7)_2(\text{SO}_4)_2(\text{H}_2\text{O})$ (b) and $\text{Hg}_3(\text{Te}_3\text{O}_8)(\text{SO}_4)$ (c).

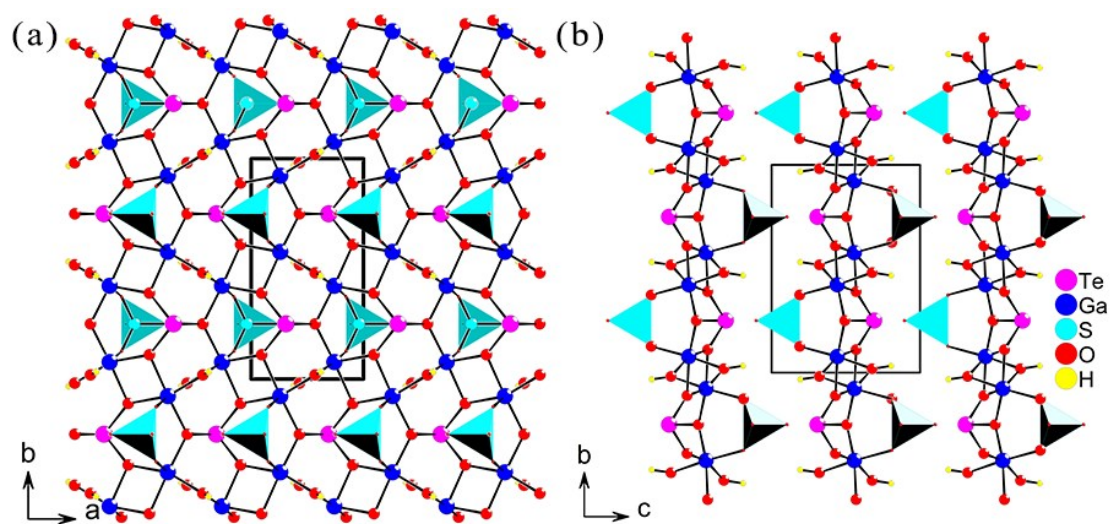


Figure S2. View of the layered structure of $\text{Ga}_2(\text{TeO}_3)(\text{SO}_4)(\text{OH})_2$ along c- (a) and a-axis (b).

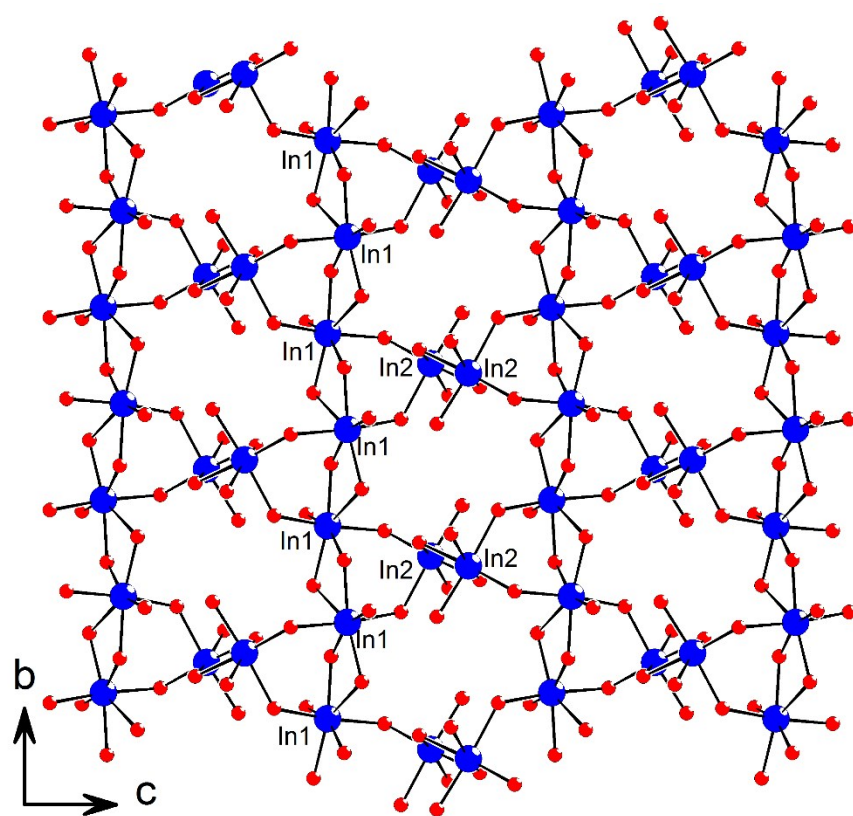


Figure S3. The indium oxide layer of $\text{In}_2(\text{TeO}_3)_2(\text{SO}_4)(\text{H}_2\text{O})$.

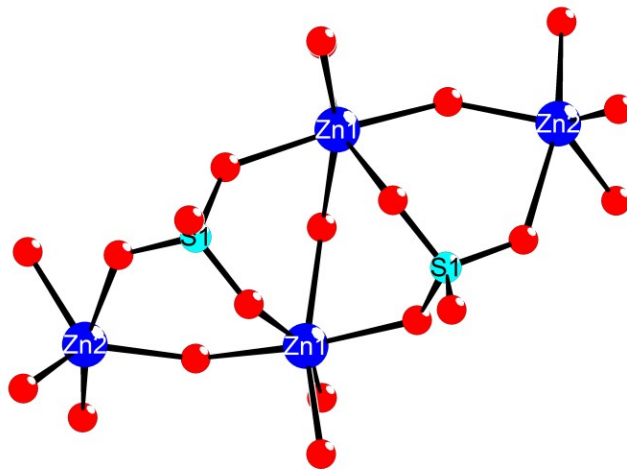
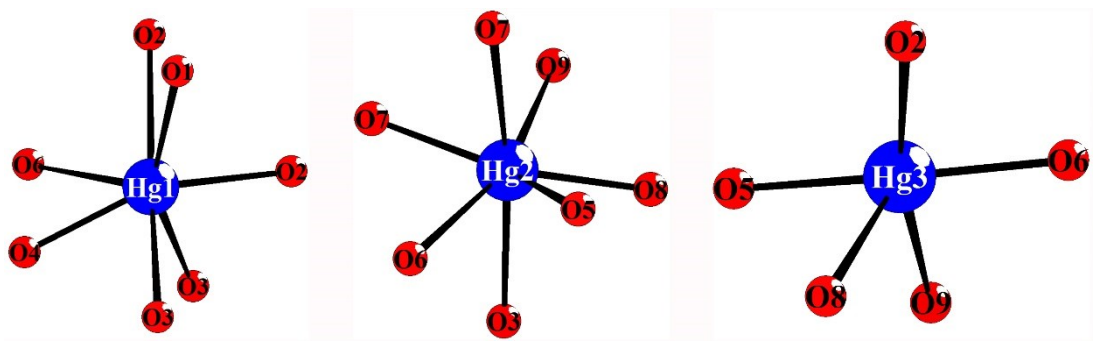
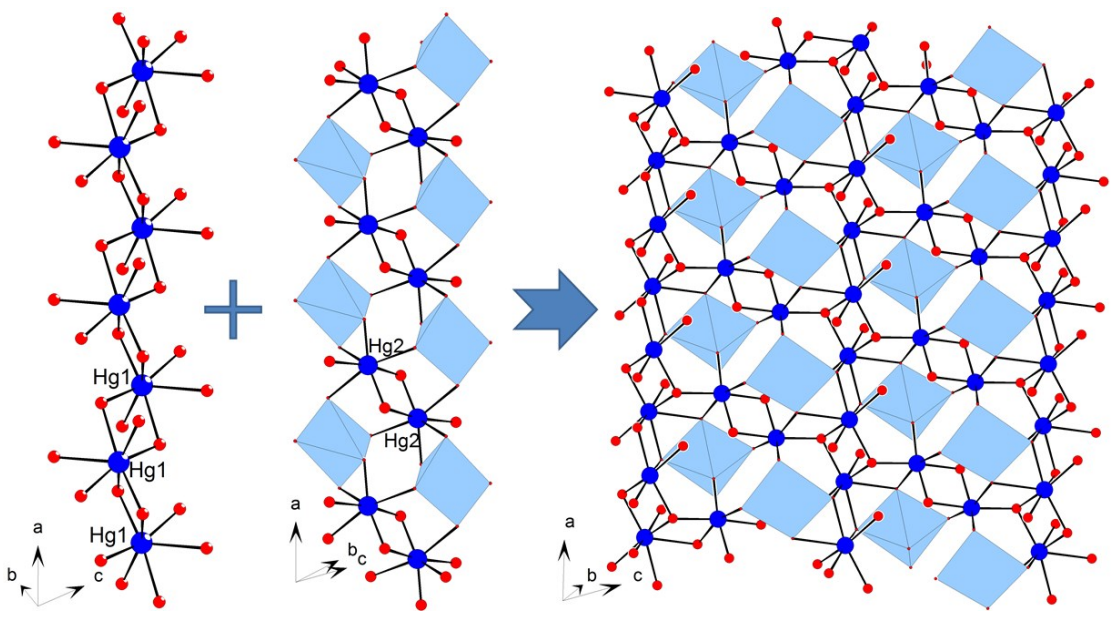


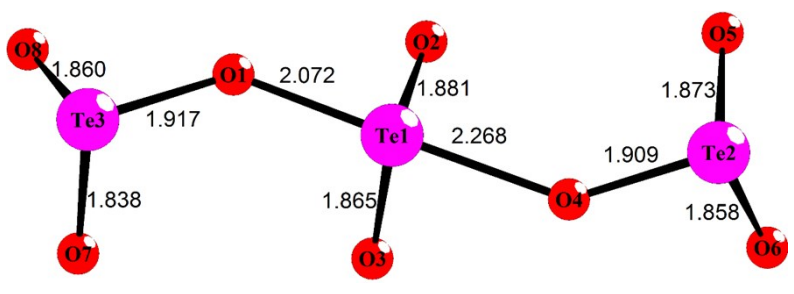
Figure S4. The $[\text{Zn}_4(\text{SO}_4)_2(\text{H}_2\text{O})]^{4+}$ cluster in $\text{Zn}_4(\text{Te}_3\text{O}_7)_2(\text{SO}_4)_2(\text{H}_2\text{O})$.



(a)



(b)



(c)

Figure S5. The coordination modes of Hg(1), Hg(2) and Hg(3) (b), the Te_3O_8 trimer (a), and the mercury oxide chains and layer (c) of $\text{Hg}_3(\text{Te}_3\text{O}_8)(\text{SO}_4)$.

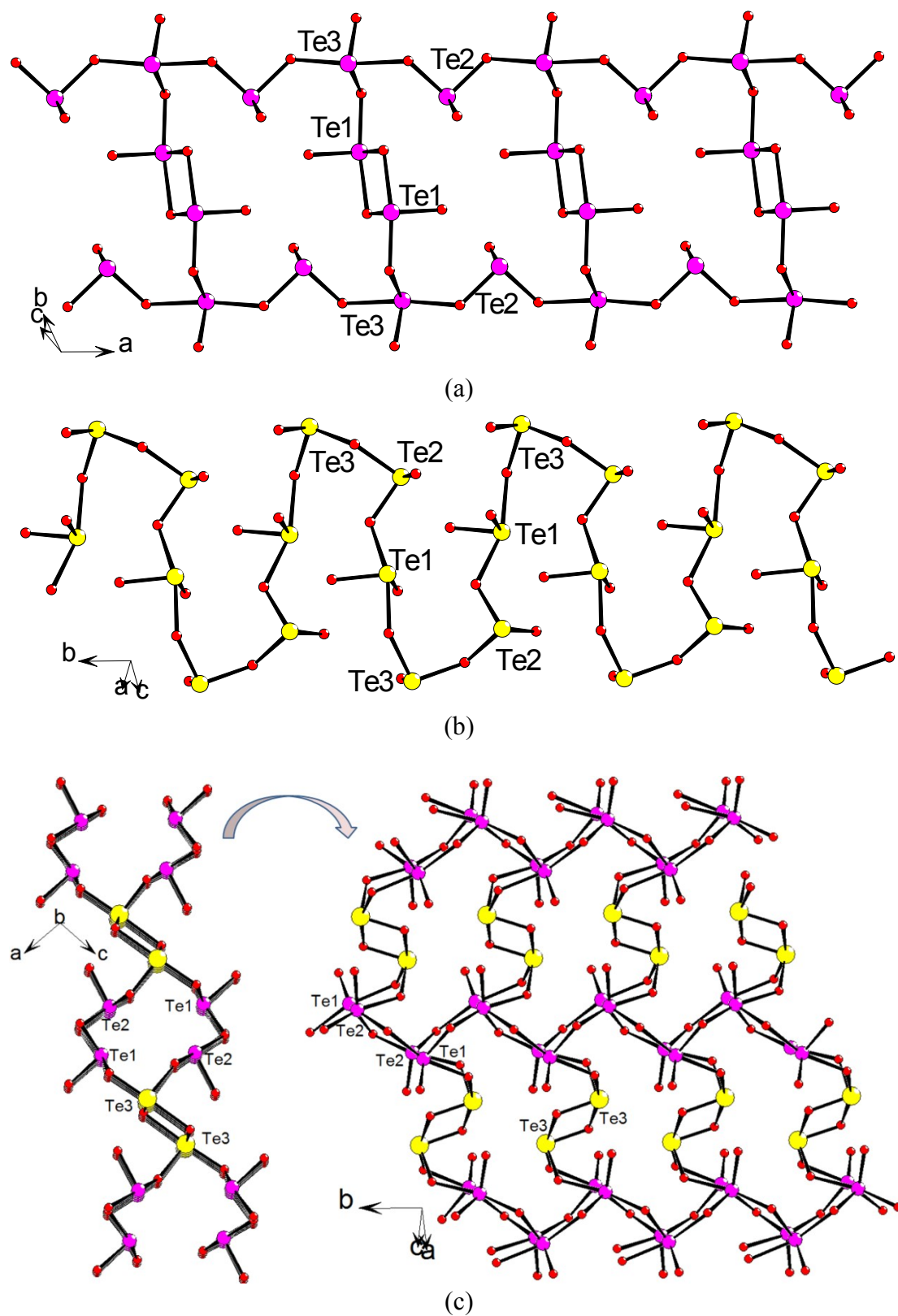
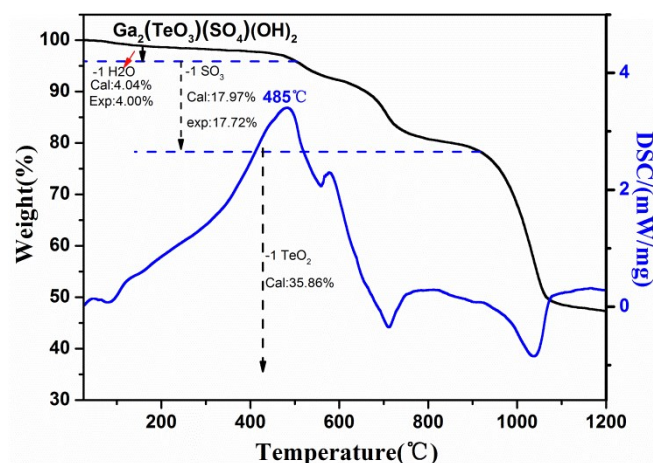
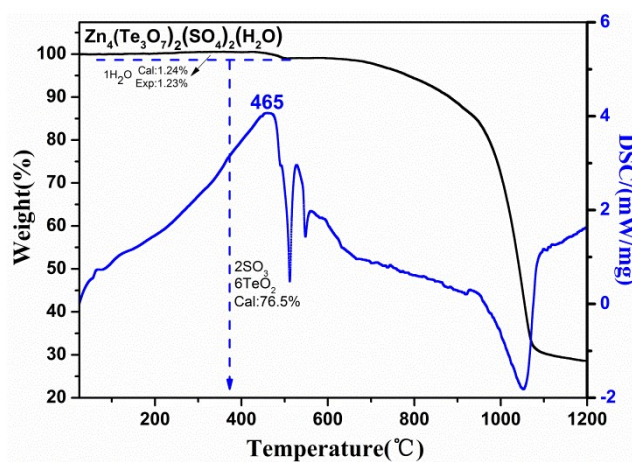


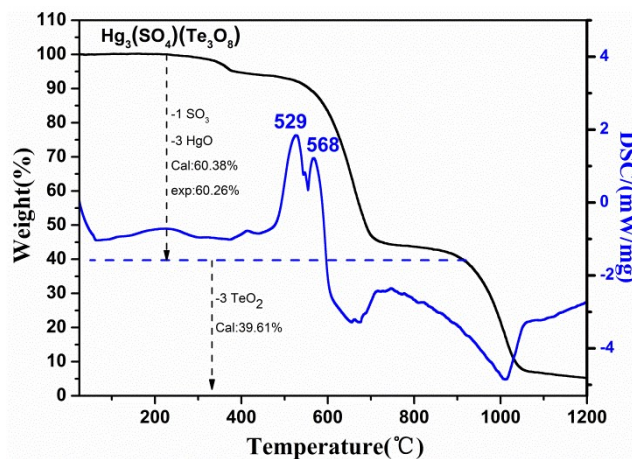
Figure S6. The ladder-shaped double chain structure in $\text{Tl}_2(\text{Te}_3\text{O}_7)$ (a), the zigzag chain in $\text{Fe}(\text{Te}_3\text{O}_7)\text{X}$ ($\text{X} = \text{Cl}, \text{Br}$) (b), the 2D layered structure in $\text{Ba}(\text{Te}_3\text{O}_7)$ (c).



(a)

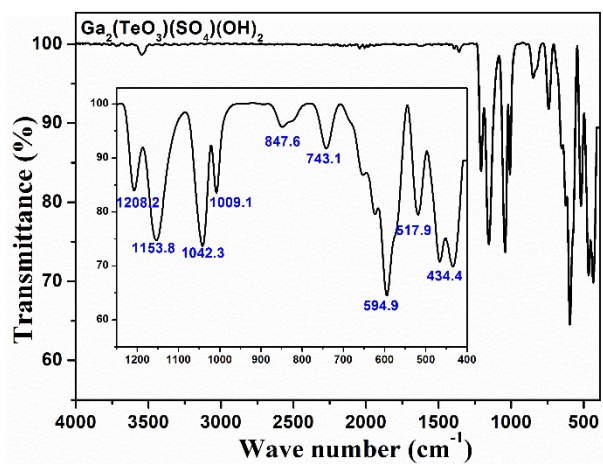


(b)

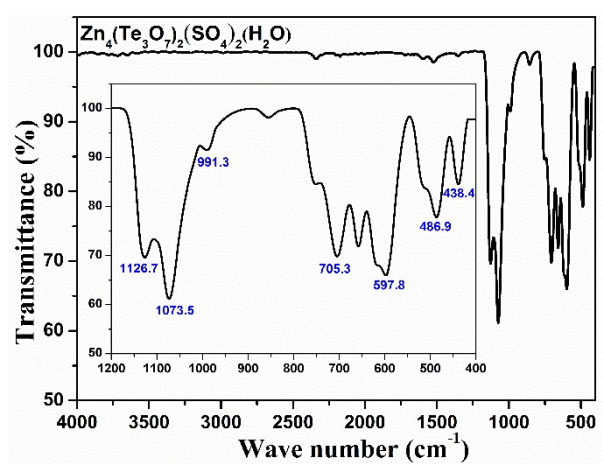


(c)

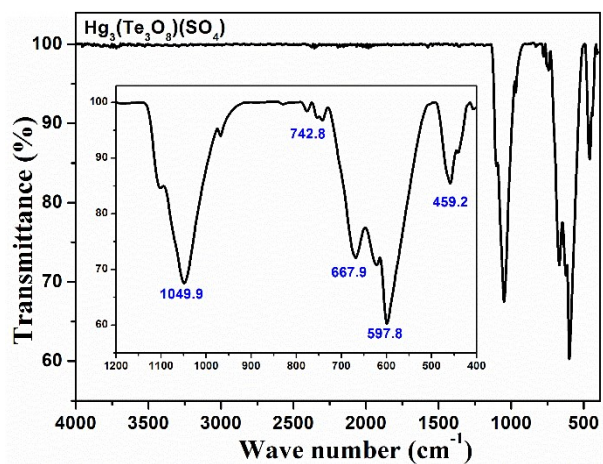
Figure S7. TGA and DSC curves of $\text{Ga}_2(\text{TeO}_3)(\text{SO}_4)(\text{OH})_2$ (a), $\text{Zn}_4(\text{Te}_3\text{O}_7)_2(\text{SO}_4)_2(\text{H}_2\text{O})$ (b) and $\text{Hg}_3(\text{Te}_3\text{O}_8)(\text{SO}_4)$ (c).



(a)

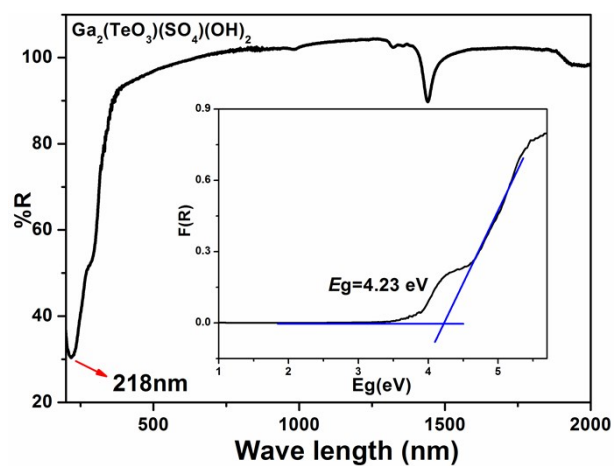


(b)

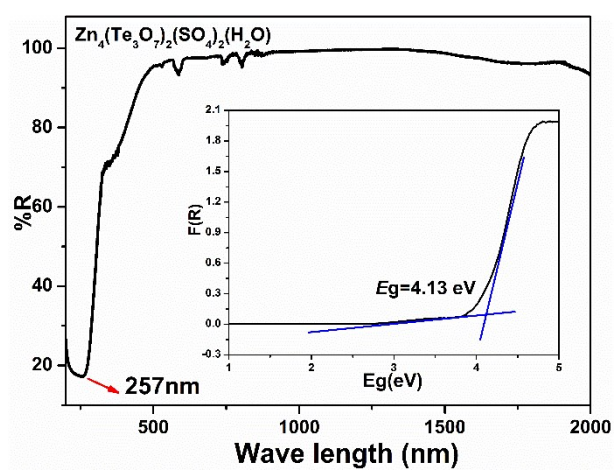


(c)

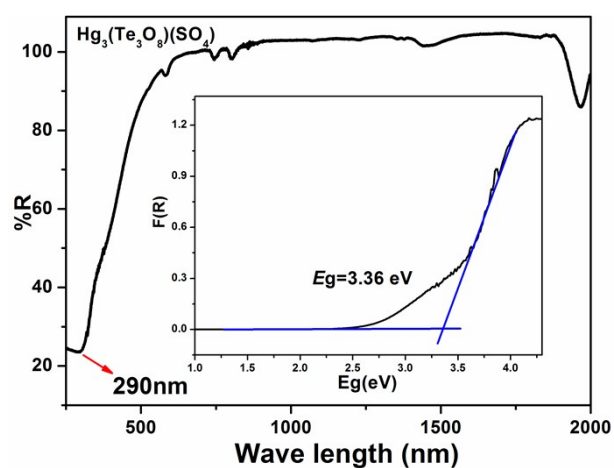
Figure S8. IR spectra of $\text{Ga}_2(\text{TeO}_3)(\text{SO}_4)(\text{OH})_2$ (a), $\text{Zn}_4(\text{Te}_3\text{O}_7)_2(\text{SO}_4)_2(\text{H}_2\text{O})$ (b) and $\text{Hg}_3(\text{Te}_3\text{O}_8)(\text{SO}_4)$ (c).



(a)



(b)



(c)

Figure S9. UV–Vis–NIR diffuse reflectance spectrum of $\text{Ga}_2(\text{TeO}_3)(\text{SO}_4)(\text{OH})_2$ (a), $\text{Zn}_4(\text{Te}_3\text{O}_7)_2(\text{SO}_4)_2(\text{H}_2\text{O})$ (b) and $\text{Hg}_3(\text{Te}_3\text{O}_8)(\text{SO}_4)$ (c).

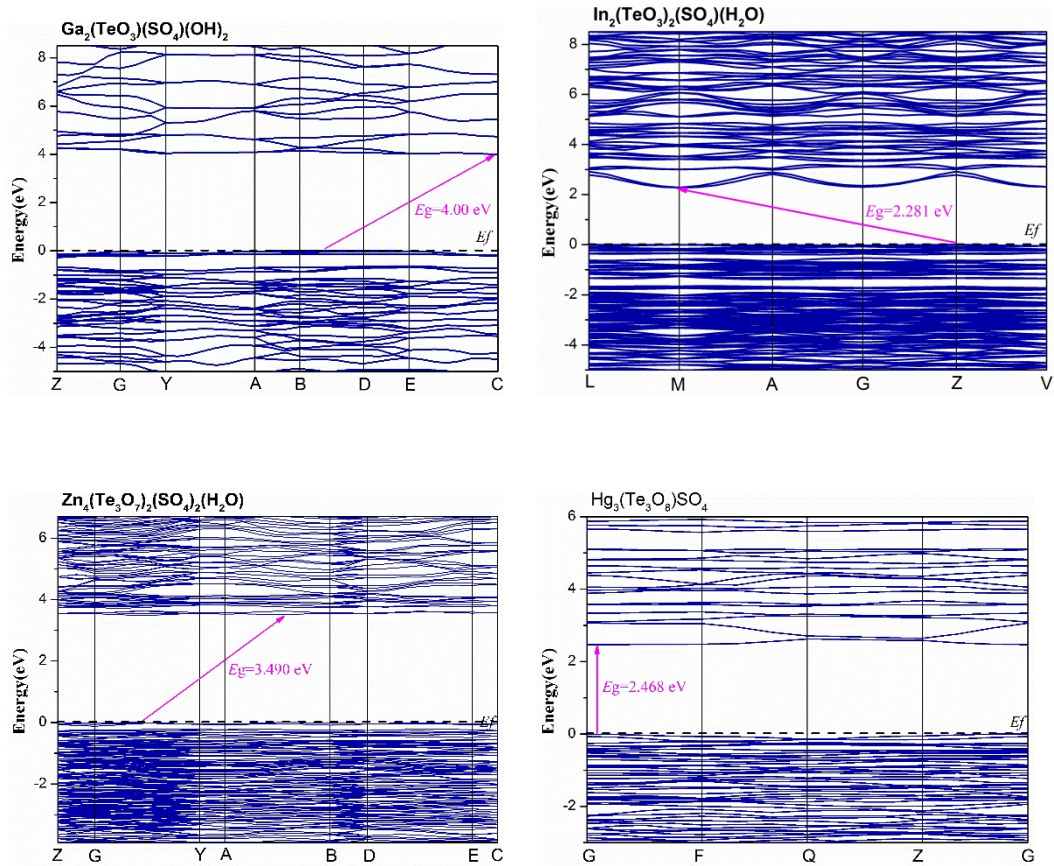


Figure S10. Calculated band structures of the four compounds.

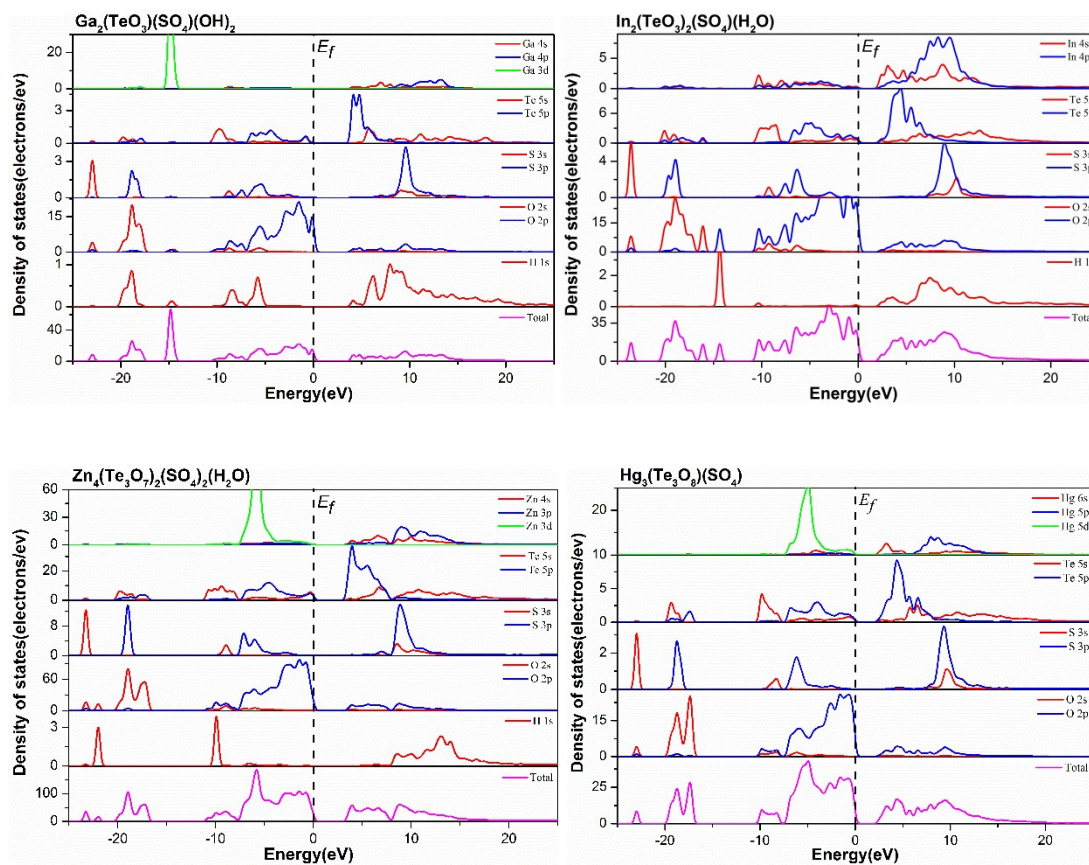


Figure S11. Calculated total and partial density of states for the four compounds.

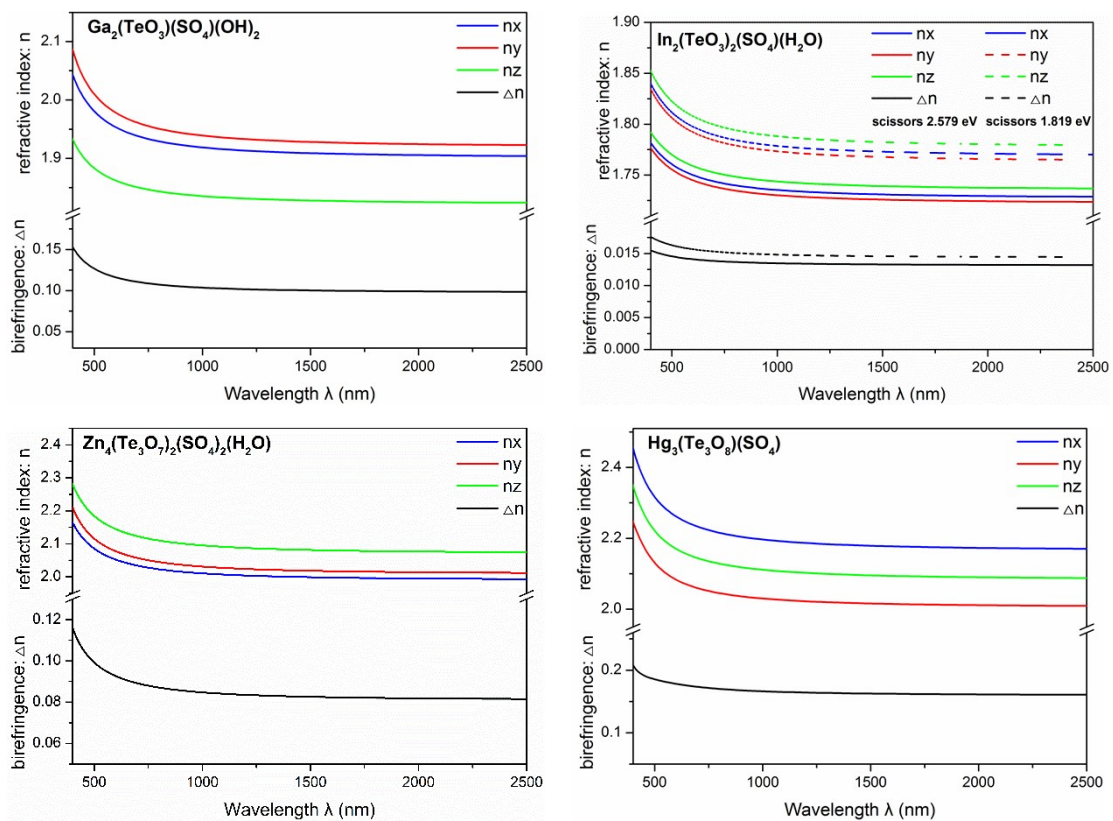


Figure S12. Calculated refractive indices and birefringence of the four compounds.

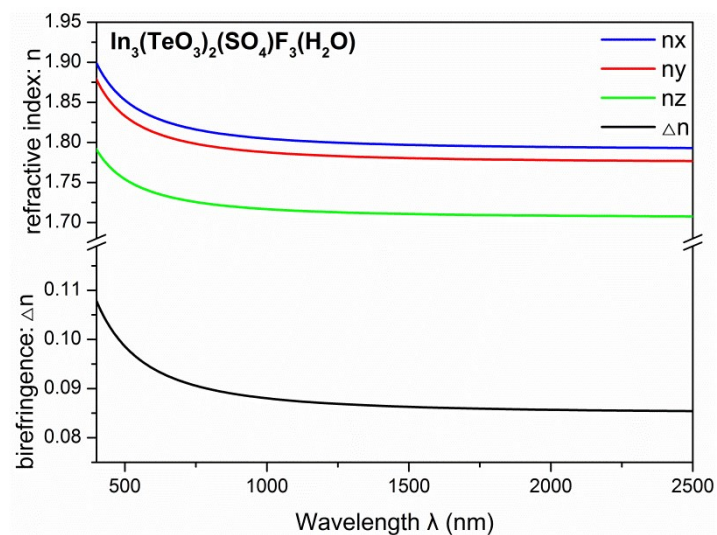
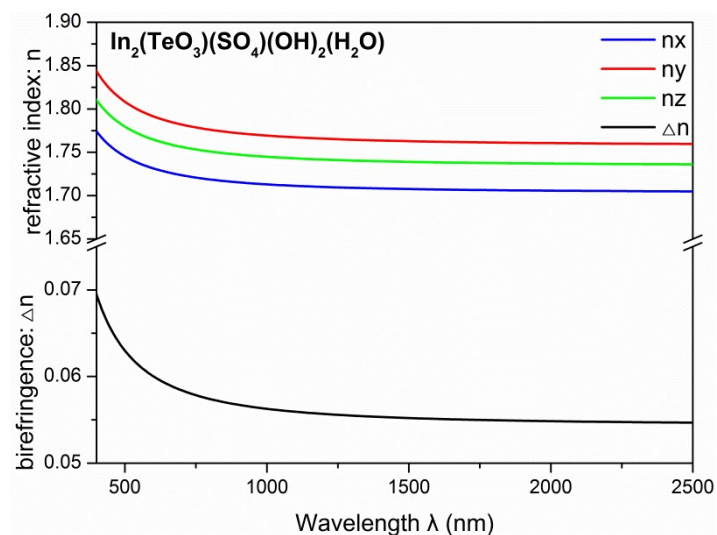


Figure S13. Calculated refractive (n) and birefringence (Δn) indices of $\text{In}_2(\text{TeO}_3)(\text{SO}_4)(\text{OH})_2(\text{H}_2\text{O})$ and $\text{In}_3(\text{TeO}_3)_2(\text{SO}_4)\text{F}_3(\text{H}_2\text{O})$.

References

- [1] M. D. Segall, P. J. D. Lindan, M. J. Probert, C. J. Pickard, P. J. Hasnip, S. J. Clark and M. C. J. Payne, First-principles simulation: ideas, illustrations and the CASTEP code, *Phys-Condens Mat.*, 2002, **14**, 2717.
- [2] V. Milman, B. Winkler, J. A. White, C. J. Pickard, M. C. Payne, E. V. Akhmatkaya and R. H. Nobes, Electronic structure, properties, and phase stability of inorganic crystals: A pseudopotential plane-wave study, *Int. J. Quantum. Chem.*, 2000, **77**, 895-910.
- [3] J. P. Perdew, K. Burke and M. Ernzerhof, Generalized Gradient Approximation Made Simple, *Phys. Rev. Lett.*, 1996, **77**, 3865.
- [4] S. Saha and T. P. Sinha, Electronic structure, chemical bonding, and optical properties of paraelectric BaTiO₃, 2000, **62**, 8828-8834.